

A modified slow sand filtration system of epikarst spring water in karst mountainous areas, China

Yuewen Zhao, Xiuyan Wang, Juan Yang, Changli Liu and Shuaiwei Wang

ABSTRACT

Epikarst springs are commonly used for drinking water in karst mountainous areas, but they tend to bring health risks to residents because of their vulnerability. In this work, a modified slow sand filtration system (M-SSF) was established as a case study to purify and conserve the epikarst spring water. The outcomes indicate that the purification of M-SSF relies mainly on the adsorption and ion exchange of the filter medium (mixtures of heat-treated red clay and crushed limestone, MHRCL) during the schmutzdecke juvenility, and on the schmutzdecke-formed food chain of pollutants → bacteria → protozoa after the schmutzdecke maturity. The closed water cellar lined with ceramic tiles could reduce the deterioration of epikarst spring water during storage. Via 16S rRNA sequencing, it was found that the high abundance of *TM6_Dependentiae* in purified epikarst spring water (PESW) suggested that the M-SSF system relies on the formation of a closed food chain to achieve effective water purification. The decrease of *Pseudarcicella* abundance in PESW indicated that M-SSF could effectively prevent the water quality from external influences represented by leeches. Besides, the 16S function prediction was used to qualitatively characterize microbial nitrogen metabolism, as well as organic matter degradation in water purification.

Key words | 16S rRNA sequencing, bacterial community structure, epikarst spring, schmutzdecke, slow sand filtration

HIGHLIGHTS

- The quality of epikarst spring water was significantly improved using the M-SSF.
- *TM6_Dependentiae* indicated that the purification of M-SSF relies on the establishment of a closed food chain.
- The M-SSF could prevent the purified epikarst spring water from being influenced by external pollution.

Yuewen Zhao

Xiuyan Wang (corresponding author)

Juan Yang

Changli Liu

Shuaiwei Wang

Institute of Hydrogeology and Environmental Geology, Chinese Academy of Geological Sciences,

No. 268 North Zhonghua Street, Xinhua District, Shijiazhuang 050061, China

E-mail: wxiuyan9948@163.com

Yuewen Zhao

Xiuyan Wang

Shuaiwei Wang

Key Laboratory of Groundwater Sciences and Engineering, Ministry of Natural Resources,

No. 92 East Zhongshan Road, Zhengding County, Shijiazhuang 050899, China

Yuewen Zhao

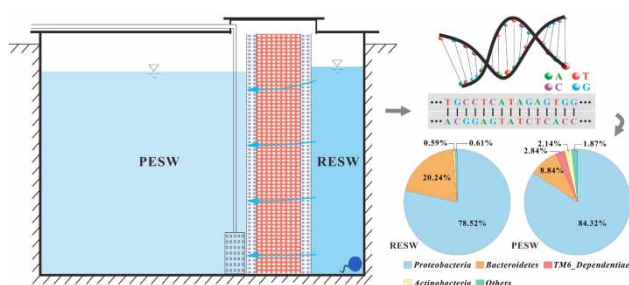
State Key Laboratory of Biogeology and Environmental Geology, China University of Geosciences,

No. 388 Lumo Road, Hongshan District, Wuhan 430074, China

This is an Open Access article distributed under the terms of the Creative Commons Attribution Licence (CC BY-NC-ND 4.0), which permits copying and redistribution for non-commercial purposes with no derivatives, provided the original work is properly cited (<http://creativecommons.org/licenses/by-nc-nd/4.0/>).

doi: 10.2166/wh.2021.242

GRAPHICAL ABSTRACT



INTRODUCTION

Karst mountainous areas are typically characterized by a large topographic relief, deep cutting depth, and rapid runoff of surface water and groundwater. Due to topographic and geological characteristics, karst mountainous areas tend to have extremely poor conditions for the construction of reservoirs, resulting in severe losses of water resources (Jiang *et al.* 2008; Wu *et al.* 2009; He *et al.* 2018). In this way, residents often experience water shortages in their daily lives, despite the moist climatic conditions of karst mountainous areas (Wang *et al.* 2005). As an important regulation and storage system, the epikarst zone can increase infiltration recharge and also delay the loss of water resources in a karst system after rainfall and, therefore, has significant functions for maintaining local water availability (Trček 2006; Hu *et al.* 2015; Champollion *et al.* 2018). Furthermore, epikarst springs usually have high outcropping positions and are easily exploited, as well as being widely distributed and suitable for meeting the dispersed domestic water demands, which can be valuable water supply sources for karst mountainous areas (Williams 2008).

In most cases, epikarst springs have shallow circulation depths (around 10 m). Their catchments typically have small areas and are covered by a thin soil layer with poor continuity, and a considerable portion of the bedrock is typically exposed (Li *et al.* 2007). Therefore, epikarst springs are very sensitive to environmental changes, such as rainfall and changes in land-use types, as demonstrated by a high vulnerability (Bakalowicz 2004; Pipan *et al.* 2018). Importantly, as cultivated land resources are generally scarce in karst mountainous areas, epikarst spring catchments are

usually relatively fertile areas where human activities are concentrated, thus increasing the risk of pollution in epikarst spring water. The reverse succession of karst habitat is not conducive to inhibiting the migration of pollutants to the epikarst springs (Sun *et al.* 2019). The soil erosion also aggravates the rocky desertification of epikarst spring catchments, increasing the health risk of epikarst spring water (Zhao *et al.* 2018).

In addition, epikarst springs show notable seasonality so that water cellars are typically constructed for epikarst springs to store water (Ren *et al.* 2018). However, epikarst spring water usually directly enters these constructed water cellars without prior treatment, and the water quality further deteriorates during the storage process. Affected by agricultural and domestic pollution sources, water contamination primarily manifests as nitrate, turbidity, and microbial indicators exceed the guidelines for drinking water quality (WHO).

As one of the earliest water treatment processes, slow sand filtration (SSF) has aroused renewed interest in its application over the past three decades due to its lack of need for chemical additives, low energy consumption, and ease of operation and maintenance (Ellis & Aydin 1995; Weber-Shirk & Dick 1999; Devadhanam Joubert & Pillay 2008; Jenkins *et al.* 2011; Haig *et al.* 2014; Lautenschlager *et al.* 2014; Zipf *et al.* 2016; Oh *et al.* 2018). Water purification by SSF is primarily attributed to several microbially mediated processes, such as predation, adsorption, and bio-oxidation (Haig *et al.* 2011, 2015; Oh *et al.* 2018), which mainly occur in the schmutzdecke with active microbial

aggregates on the SSF surface. Conventional SSF schmutzdecke requires 20–40 days to reach maturity (D'Alessio et al. 2015; Fish et al. 2017), while SSF with juvenile schmutzdecke could not achieve an ideal treatment effect. To reduce the cost of purification materials and overcome the sub-optimal performance during schmutzdecke juvenility, the mixtures of heat-treated red clay and crushed limestone (MHRCCCL) modified SSF (M-SSF) in this study were used for purifying the epikarst spring water in karst mountainous areas. A closed water cellar lined with ceramic tiles was used to store the purified epikarst spring water (PESW), aiming at preventing PESW from deterioration during storage. The high-throughput sequencing was used to study the relationship between water purification and the bacterial community structure, and then, the purification mechanism of the M-SSF system of epikarst spring water were discussed.

MATERIALS AND METHODS

Site description

The target epikarst spring is located in the east of the Xiaojiang River Basin and affiliated with Ading Village, Luxi County, Yunnan Province (Figure 1). The catchment of Ading Epikarst Spring (AES) is a typical mountainous area in the outer margin of the karst fault basin, with an altitude of 2,288 m, and has a subtropical plateau monsoon climate, with an annual average temperature of 13.0 °C and annual average rainfall of 1,200 mm. However, rainfall is extremely unevenly distributed in time, with rainfall between May and October accounting for about 85% of the total for the year. The formation of lithology in Ading Village is dominated by the limestone, dolomite, and mudstone of the Middle Triassic epoch. The burial depth of saturated water in Ading Village is more than 100 m, which is not suitable for well development and utilization (Figure 2). AES is developed in argillaceous dolomite, and its flow rate is small with obvious dynamic variations, which are approximately 0.15 L/s during the wet season and 0.08 L/s during the dry season. The soil type of AES catchment is carbonate red soil, and the soil layer is shallow with a thickness generally less than 0.3 m. The land-use

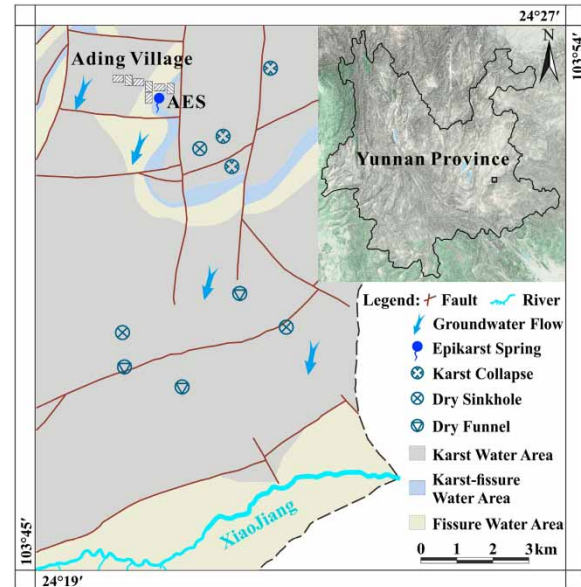


Figure 1 | Karst geological conditions in the area where the AES is located. The karst geological schematic map includes part of the mountainous area and the river valley in the east of Xiaojiang basin. The black square in the topographic image shows the scope of the karst geological schematic map in Yunnan Province.

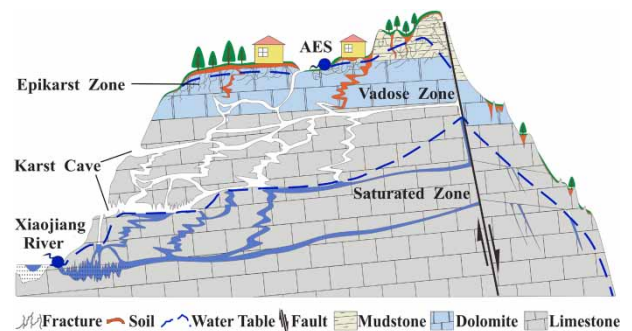


Figure 2 | Schematic diagram of the karst geological profile in the area where the AES is located.

types of AES catchment are villages and cultivated land, and the spring water quality is hence affected by pollution from agriculture, animal husbandry, and domestic sewage. The AES water is stored in cement-lined open water cellars, which are highly susceptible to external influences (including plant litter, animal excrement, and human pollution), and the water quality is easily deteriorated. The prior water quality test results of raw epikarst spring water (RESW) have shown that sensory indicators and microbial indicators in the water have partly exceeded the guidelines for drinking water quality (WHO) or

standards for drinking Water Quality of China (GB 5749-2006) (Supplementary Table S1).

Establishment of the M-SSF system

The M-SSF system was established 1 m away from the AES (Supplementary Figure S1) during the dry season when the epikarst zone had the lowest water table (0.8 and 0.1 m during the wet season). It was lined with bricks and cement, leaving a groundwater outlet at the bottom, and ceramic tiles adhered to the inner wall. Previous studies have shown that the ceramic tile lining can decrease the hardness and total dissolved solids of cellar water, and can also reduce the attachment and growth of microorganisms compared with the cement lining (Zou *et al.* 2007). According to the investigation, residents' daily water consumption of AES was usually below 2 m³/day, hereby the size of the M-SSF system was designed (Figure 3). The slow sand filtration barrier (SSFB) of this system used a side colonization mode, which consisted of schmutzdecke colonization, adsorption layer, and supporting layer, and a stainless-steel cage and nylon filter cloth to be modularized for ease of cleaning and replacing. Both the supporting layer and the schmutzdecke colonization were filled with SiO₂ particles (0.15–0.18 mm, analytical reagent) using for supporting and immobilizing the adsorption layer. The SiO₂ particles were chemically stable and suitable for microbial colonization without affecting the water quality. The adsorption layer was comprised of the MHRCCCL. Red clay was collected at a local uncontaminated woodland area (0.5–1 m) and was air-dried and milled into a size of 300-mesh, and

then heat-treated at a temperature of 300 °C in a muffle furnace for 3 h under anaerobic conditions (Neytech, USA). Previous studies have shown that heat-treatment with 300 °C could sterilize both bacteria and fungi in soil effectively, and increase the specific surface area and cation exchange capacity and then enhance the adsorption capacity of clay (Duane & Wolf 1994; Guerrero *et al.* 2005; Chen *et al.* 2011). Crushed limestone was sifted within a narrow range of particle sizes (0.5–2 mm), elutriated, and then sterilized at a temperature of 300 °C for 3 h under anaerobic conditions (Neytech, USA). The grain size analyses and costs of red clay and crushed limestone are shown in Supplementary Table S2. Then, heat-treated red clay and crushed limestone were mixed thoroughly at a volume ratio of 4:7 and then compacted to a density of 1.75 g/cm³ aiming at making the adsorption layer with a reasonable permeability (≈ 0.2 m/h). In this condition, even under the maximum daily water consumption (2 m³/day, the head difference on both sides of SSFB is 0.83 m), the filtering velocity of SSFB in this study still meets the velocity limit range of SSF (<0.6 m/h), which could ensure the purifying effect (Zhu 2014).

Sample collection and testing

Based on the water quality test results of RESW both in the wet and dry seasons in 2017 (Supplementary Table S1), some indicators of RESW that had been found to pose potential health risks were monitored to research the purifying effect of the M-SSF system (Table 1). These indicators of RESW and PESW were monitored for 360 days from 26

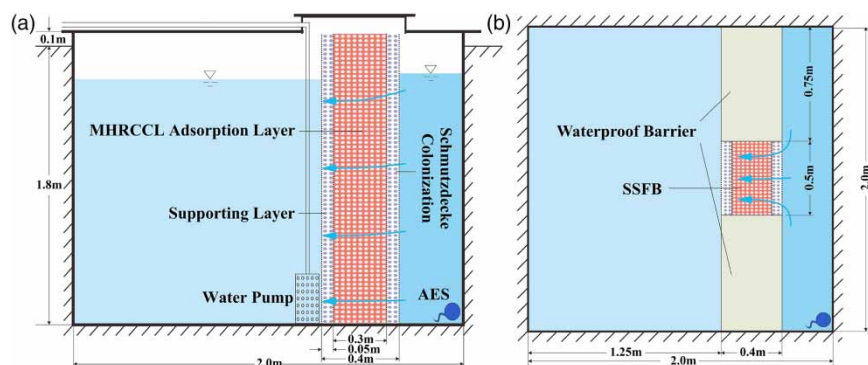


Figure 3 | Structural schematic diagram for the M-SSF system: (a) the profile schematic diagram of the M-SSF system and (b) the plane schematic diagram of the M-SSF system.

Table 1 | Comparison of the representative water quality parameters of the PESW and the RESW on days 2, 5, 10, 20, 40, 90, 180, and 360

Samples	HPC CFU/mL	Total coliforms MPN/100 mL	Thermotolerant coliforms	<i>E. coli</i>	Visible to the naked eye –	Chromaticity °	Turbidity NTU	pH –	COD mg/L	NH ₃ (N) mg/L	NO ₃ ⁻ mg/L
RESW Day 2	180	540	240	79	Russet precipitation	5	1.04	7.79	1.13	0.57	55.39
PESW	110	0	0	0	ND	<5	0.75	7.50	0.75	0.05	25.77
RESW Day 5	640	350	170	49	Russet precipitation	<5	1.02	7.74	1.07	0.48	50.52
PESW	360	8	5	5	ND	<5	0.81	7.52	1.02	0.19	30.69
RESW Day 10	260	540	140	94	Russet precipitation	5	1.01	7.77	1.10	0.42	46.81
PESW	420	5	2	0	ND	<5	0.72	7.49	1.04	0.08	23.60
RESW Day 20	2,500	1,600	1,600	1,600	Russet precipitation	5	1.17	7.79	1.14	0.51	53.58
PESW	400	0	0	0	ND	<5	0.69	7.50	0.90	0.07	21.21
RESW Day 40	2,240	920	220	94	Suspended solids	5	1.13	7.67	1.63	0.59	62.35
PESW	480	0	0	0	ND	<5	0.58	7.52	0.88	0.03	23.34
RESW Day 90	1,740	1,600	920	180	Suspended solids	<5	1.11	7.64	1.60	0.57	59.39
PESW	99	0	0	0	ND	<5	0.66	7.53	1.10	0.02	23.87
RESW Day 180	370	110	23	13	ND	<5	0.67	7.78	1.22	0.32	44.20
PESW	220	0	0	0	ND	<5	0.54	7.65	1.05	0.04	24.61
RESW Day 360	590	430	180	180	Russet precipitation	<5	0.96	7.59	1.06	0.44	55.40
PESW	380	0	0	0	ND	<5	0.77	7.43	0.93	0.04	22.03

ND, Not detected.

May 2018. RESW and PESW samples (0.25 L for microbiological testing and 1.5 L for hydrochemical testing) were taken on days 2, 5, 10, 20, 40, 90, 180, and 360, and were stored in a cooler (4 °C) during transportation and then tested immediately (<24 h). Total coliforms, thermotolerant coliforms, and *E. coli* were enumerated using a multiple tube fermentation method, whereas heterotrophic plate counts (HPC) were assessed by a pour plate method. Additionally, the pH of these samples was measured using a SevenCompact pH meter (Mettler Toledo, Switzerland); turbidity and chromaticity were measured using a turbidity meter and a chromaticity meter, respectively (Hach, USA); nitrate was measured with an ion chromatograph (Dionex, USA); chemical oxygen demand (COD) and ammonia were measured with a spectrophotometer (Hach, USA). During the COD test, samples were digested (105 °C) in advance by a special reagent based on permanganate (Lianhua Technology Co., Ltd, China). Following digestion, samples were measured in a 30 mm cuvette with a light wavelength of 510 nm. During the measurement of ammonia, samples were pretreated with Nessler's reagent and then measured in a 10 mm cuvette at a light wavelength of 420 nm.

In addition, as schmutzdecke usually matures within days 20–40 (D'Alessio *et al.* 2015; Fish *et al.* 2017), samples of 16S rRNA gene sequencing were collected for the RESW and the PESW water samples on day 40 of M-SSF system operation. 5-L water samples were filtered using a 0.22-µm microporous membrane (47 mm diameter, Millipore, USA) to extract microorganisms in the water. The microorganism-enriched membrane was stored using dry ice during transportation (–78.5 °C) and sent for testing immediately. The V4–V5 hypervariable region of the bacterial 16S rRNA gene was amplified using the universal primer 515F (GTGC CAGCMGCCGCGG)/R907 (5CCGTC AATTCMTT-TRAGTT) (Mi *et al.* 2015), and the samples were sequenced using the Illumina MiSeq platform. The sequencing data could be found on the NCBI database (ID: PRJNA689665).

Data analysis

Bacterial sequences were clustered into operational taxonomic units (OTUs) with a maximum distance of 3% by the UPARSE pipeline (Edgar 2013). Using the SILVA database (silva128/16S_bacteria), sequences were phylogenetically

assigned to phylum, class, and other taxonomic levels by MOTHUR. The relative abundance of a given phylogenetic group was then calculated. Based on these data, the circos diagram was made by R. Based on PICRUSt, the 16S function prediction for the RESW and the PESW are as follows. The effect of the number of copies of the 16S marker gene in the genome of the species was removed, then each OTU was compared with the clusters of orthologous groups (COG) and the Kyoto Encyclopedia of Genes and Genomes (KEGG) to obtain the COG family information or the KEGG orthology information corresponding to the OTU. Then, the COG and pathway abundances were calculated.

RESULTS AND DISCUSSION

M-SSF system effects

The M-SSF system operation started at the beginning of the wet season, at this time, the water table in the epikarst zone was low. With an increase of precipitation, the water table of the epikarst zone was raised by a large margin in the rainy season. The recharge of epikarst water by precipitation also aggravated the pollution of RESW (Table 1), which showed increases in turbidity, COD, HPC, coliforms, and

so on. Because of the land-use types of the AES catchment dominated by residential and cultivated land, the farmyard manure and household waste had been accumulated in the soil during the dry season. With the rainy season beginning, the rainfall mobilized these accumulated pollutants in the soil to the epikarst water, which suggested that the thin soil layer in the epikarst zone could not protect the epikarst spring water from pollution effectively. Further analysis showed that HPC, coliforms, and turbidity of the RESW reached their peak on day 20, while ammonia, nitrate, and COD reached their peak on day 40 (Table 1). These results agree with other studies in which particulates arrive prior to solutes on account of the exclusion process, which occurs in fissure flows of epikarst zones (Pronk *et al.* 2009; Savio *et al.* 2019; Bandy *et al.* 2020). Moreover, the pH of the RESW decreased slightly, which could be attributed to the dilution effect of rainfall (He & Li 2005).

In contrast to the RESW, the water quality of the PESW was improved significantly (Table 1). Generally, the conventional SSF with juvenile schmutzdecke during the initial stage could not achieve the optimal performance. However, due to using MHRCCCL as the filtration medium, the M-SSF system in this study could ensure efficient purification of epikarst water with juvenile schmutzdecke (Figure 4). The M-SSF system mainly relied on the adsorption, interception,

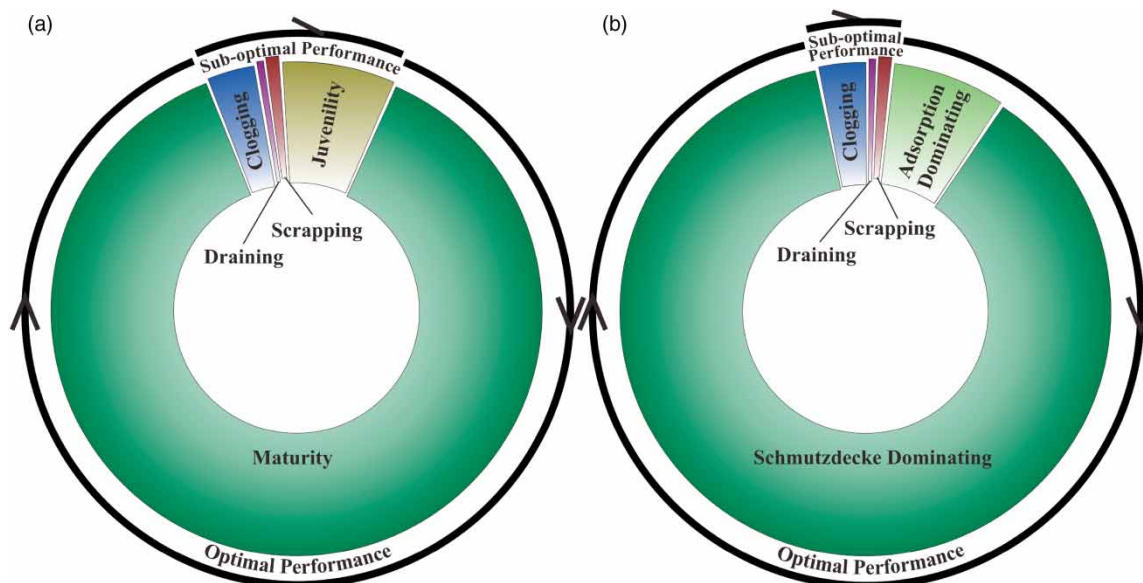


Figure 4 | Comparison between a conventional SSF and the M-SSF system: (a) the operational period of the conventional SSF and the performance of each stage and (b) the operational period of M-SSF and the performance of each stage.

and ion exchange of MHRCCCL for water purification before its *schmutzdecke* matured. Although coliforms in PESW were not removed completely on days 5 and 10, coliforms of PESW were significantly eliminated compared to RESW by the M-SSF system before its *schmutzdecke* matured. With superior specific surface area and cation exchange capacity, solutes in PESW such as nitrate and ammonia were largely purified. The M-SSF system of AES exhibited acceptable purifying effects during the adsorption dominating stage. By day 20, the *schmutzdecke* was approaching maturity, and the main mechanism of water purification in the M-SSF system shifted from adsorption dominating to microbial in *schmutzdecke* dominating. The M-SSF system relied on microbially mediated mechanisms (e.g., predation and bio-oxidation) in the *schmutzdecke* to achieve effective water purification (Bauer *et al.* 2011; Lee & Oki 2013; Haig *et al.* 2014; Oh *et al.* 2018). The purifying effect on AES water was further improved, as can be seen by the complete removal in coliforms (Table 1), suggesting that the M-SSF system achieved optimal performance during the *schmutzdecke* maturity. Over time, the biofilm got thicker and the permeability of M-SSF system decreased. It could be observed that the waterhead of both sides of SSFB changed from 5 cm (day 2) to 12 cm (day 180) and then to 21 cm (day 360). The increase of bilateral waterhead might mitigate the effect of the decreasing permeability of SSFB, so that the M-SSF system would maintain relatively stable filter flows for as long as possible. Compared with the top colonization mode of the SSFs in our previous study (Zhao *et al.* 2019), the side colonization mode tended to maintain a longer optimal performance time without easily clogging which could be attributed to the inconsistency direction of filtration and particle precipitation direction.

Furthermore, the water quality indicators of the RESW were worse in the wet season than the dry season (Supplementary Figure S2), especially HPC and coliforms in summer. Besides rainfall mobilization of accumulated pollutants in the soil, the RESW was also subject to bacteria breeding and external contaminations such as pollution from animals and humans due to its open storage mode (Ahmed *et al.* 2011; WHO 2011; Zhang *et al.* 2017). To address this problem, the storage form of water cellar in the M-SSF system was improved. By adopting a closed water storage mode using ceramic tile lining, the external contaminations

and bacteria breeding were effectively reduced. The monitoring results showed that water quality indicators of PESW were stable throughout 360 days (Table 1), indicating that the M-SSF system had the potential to prevent the water quality of the PESW from deterioration during the storage process.

Bacterial community structures of the PESW and the RESW

According to the sequencing results of 16S rRNA, the test samples all had high coverage (>99%), indicating that the test results had good representativeness. The PESW and the RESW had different degrees of variation in species taxonomy, diversity, and evenness. In terms of species taxonomy, the number of all taxonomic levels in the PESW and the RESW did not seem to have significant changes (Table 2), but there were substantial differences in species diversity and evenness between PESW and RESW. By using the Shannon diversity index as an example, the RESW (<3) was markedly smaller than the PESW (>3). According to previous research results, a Shannon diversity index of <3 indicates that β -diversity of water might be polluted in a high probability, and a Shannon diversity index of >3 indicates a high probability of β -unpolluted water (Yang *et al.* 2017). The more diverse bacterial communities, the more enriched their environmental functions are, and a higher bacterial community diversity also means enhanced stability of environmental functions. The coexistence of multiple species can provide a greater guarantee of comprehensive environmental functions; that is, when some species lose a certain environmental function under ecological pressure, other species can fill this gap of the environmental function (Wittebolle *et al.* 2009; Lautenschlager *et al.* 2014; Saifullah & Purnomo 2015; Fish *et al.* 2017). Similarly, the greater the bacterial community evenness, the better its tolerance and stability in environmental stresses. When the bacterial community evenness is low; that is, when the communities are controlled by only a few species, the resistance to disturbance can only occur when the predominant species are tolerant of disturbance (Wittebolle *et al.* 2009; Haig *et al.* 2015). In comparison, when the bacterial community evenness is high, so is the probability of the presence of species that are resistant to water quality disturbance.

Table 2 | Amounts of the different taxonomic levels, diversity indices, and evenness indices of the bacterial communities in the PESW and the RESW

Samples	Taxonomic levels										Diversity indices					Evenness indices				
	Phylum	Class	Order	Family	Genus	Species	OTU	Shannon	Simpson	Ace	Chao 1	Help	Shannonneven	Simpsonneven	Coverage					
RESW	22	37	72	121	207	275	343	2.09	0.33	466.95	479.12	0.02	0.36	0.01	99.60%					
PESW	22	35	73	121	208	271	341	3.94	0.04	400.71	410.16	0.15	0.68	0.08	99.75%					

The bacterial community structure of RESW and PESW at the phylum level was analyzed. The results show that in the RESW, *Proteobacteria*, *Bacteroidetes*, and *Actinobacteria* were the predominant phyla; however, *Proteobacteria*, *Bacteroidetes*, *TM6_Dependentiae*, and *Actinobacteria* were the predominant phyla in the PESW (Figure 5). As the denitrifier mostly exists in *Proteobacteria*, the nitrate decreasing in PESW (Table 1) may be related to the abundance of *Proteobacteria* increasing. Also, the schmutzdecke of SSF is rich in the biological population, including bacteria, protozoa, and various microbial secretions. These microbes form a virtuous food chain, and *TM6_Dependentiae* in PESW seems to be an indicator that bacterium confirms the formation of a food chain in SSF. Previous studies have found that *TM6_Dependentiae* is a type of bacterium that primarily parasitizes protozoa (e.g., heterotrophic flagellates) and lives a highly host-related lifestyle. Their genomes are small (1.0–1.5 Mb) and they lack complete biosynthetic pathways for various essential cellular building blocks, including amino acids, lipids, and nucleotides (Yun Kit Yeoh et al. 2016; Deeg et al. 2018). Furthermore, the *Chromulinavorax destructans* generated by *TM6_Dependentiae* can lyse heterotrophic protists and thus *TM6_Dependentiae* enter the water. Therefore, the high abundance of *TM6_Dependentiae* in PESW indicated that there was a high abundance of heterotrophic protists in the M-SSF (Deeg et al. 2018). As predators at the top of the SSF food chain, the heterotrophic protists were too large to pass through the SSF; however, the lysis of heterotrophic protists engaged themselves as a carbon source in the food chain and re-participated in the material cycle of the SSF. The high abundance of *TM6_Dependentiae* in PESW found in this study confirms that its host heterotrophic protists were widely present in the schmutzdecke as predators. Moreover, *TM6_Dependentiae*, an indicator bacterium, could provide evidence that the formation of a complete food chain is the main mechanism for water purification by the mature SSF.

Bacterial community structure analysis on the genus level (Figure 6) shows that the genera of RESW primarily included *Acidovorax* (54.24%), *Pseudarcicella* (17.24%), *Acinetobacter* (6.41%), and *Rhodobacteraceae* (3.93%). In particular, the abundance of *Pseudarcicella* in the RESW was 460 times that in the PESW. *Pseudarcicella* primarily parasitizes in the skin of leeches (Kampfer et al. 2012), and

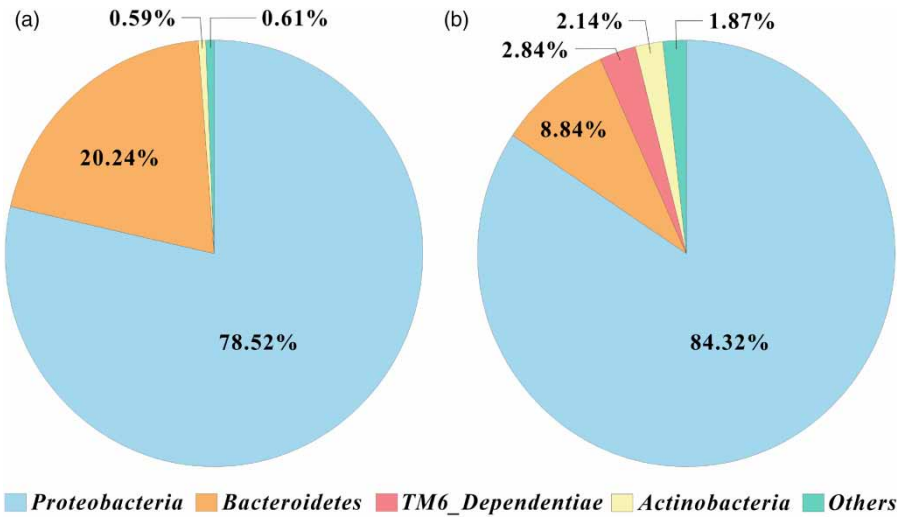


Figure 5 | Bacterial community structure analysis on the phylum level: (a) Pieplot of RESW and (b) Pieplot of PESW.

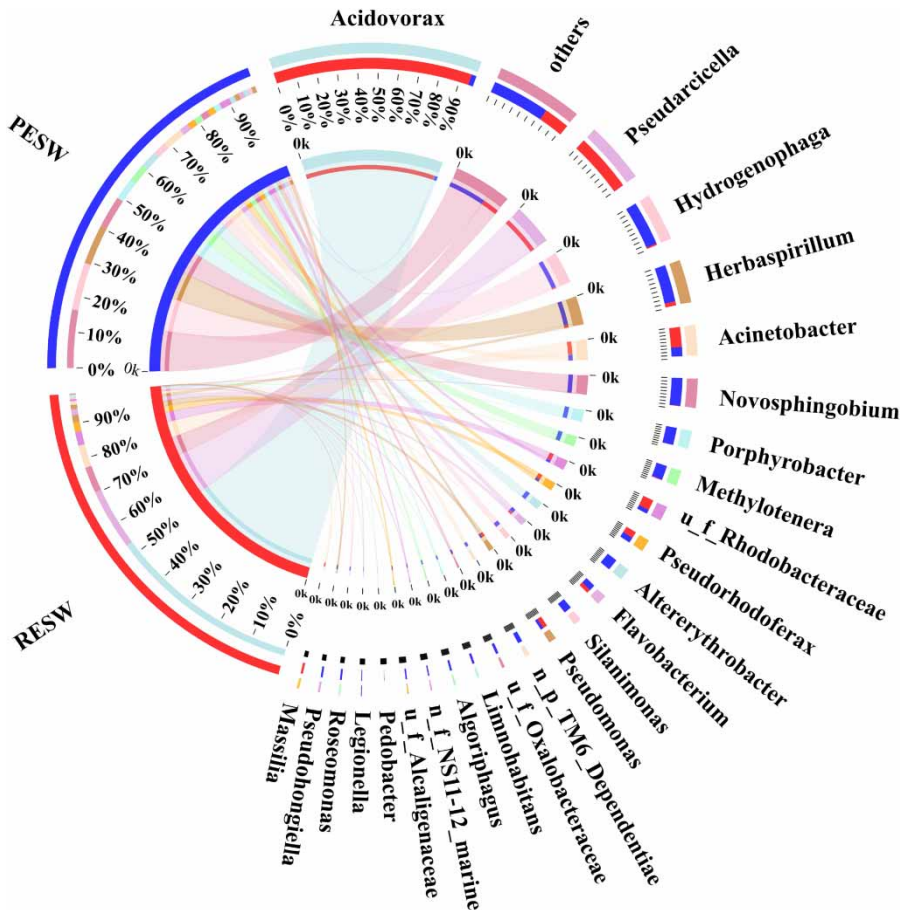


Figure 6 | Circos diagram on the genus level of the PESW and the RESW. u_f, unclassified family; n_f, no rank family; n_p, no rank phylum.

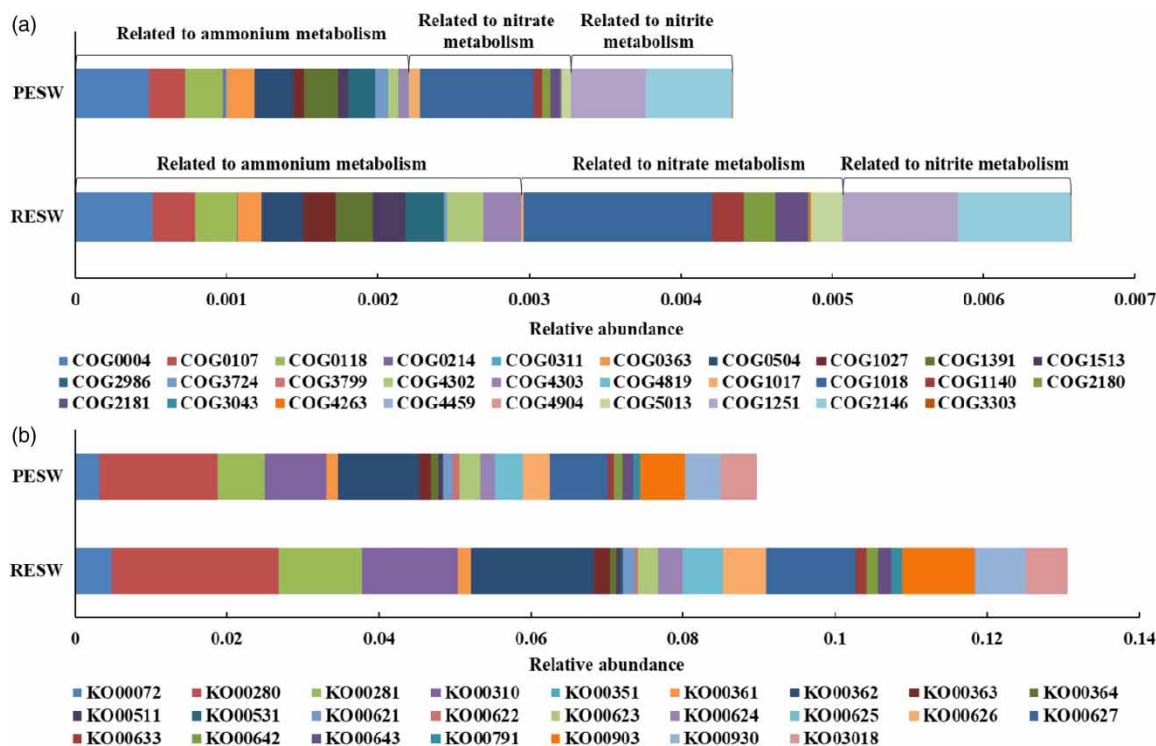


Figure 7 | Stacked bar charts of relative abundance in the PESW and the RESW based on 16S functional prediction. (a) Chart of COG related to ammonium, nitrate, and nitrite metabolism; the description of each COG is shown in Supplementary Table S1; (b) chart of pathways associated with organic pollutant degradation; the description of each pathway is shown in Supplementary Table S2.

its existence could serve as a sign that RESW is affected by external animal pollution. By contrast, *Pseudarcicella* rarely existed in the PESW, which suggested that the M-SSF system could cut off the external pollution effectively and prevent epikarst water from deteriorating during storage. The bacterial genera of the PESW primarily included *Hydrogenophaga* (13.38%), *Herbaspirillum* (11.31%), *Novosphingobium* (8.95%), *Porphyrobacter* (6.23%), *Methylotenera* (5.33%), *Altererythrobacter* (4.69%), and *Silanimonas* (3.71%). Among these bacterial genera, *Novosphingobium* can degrade aromatic compounds (Liu *et al.* 2005), and *Methylotenera* are obligate methylamine-degrading bacteria (Kalyuzhnaya *et al.* 2006). Some of these bacterial genera are related to the degradation of organic matter, as well as the removal of total nitrogen, and are primarily those that remain after water purification using the M-SSF.

Based on the results from the 16S function prediction, the COG associated with ammonia, nitrate, and nitrite were selected for analysis. It is seen from Figure 7(a) that there was a higher relative abundance of ammonia-, nitrate-, and nitrite-related COG in the RESW than in the

PESW (the definitions of COG are shown in Supplementary Table S3), suggesting a higher relative abundance of microorganisms associated with the metabolism of these nitrogen compounds in the RESW. The higher abundance of nitrogen metabolism microorganisms in the RESW suggests a greater selective pressure for nitrogen compounds to form in the RESW than in the PESW (Zelaya *et al.* 2019), which is consistent with the results of the water quality testing. Similarly, the RESW had a higher relative abundance of most of the metabolic pathways associated with the degradation of organic pollutants (Figure 7(b)), especially aromatic compounds (Supplementary Table S4), than the PESW, which is consistent with previous studies (Bai *et al.* 2013). This also implies that the RESW was more intensely affected by organic pollution, which is also consistent with the COD, as an indicator of dissolved organic pollution in these water quality tests. The results of the 16S function prediction further confirmed the effect of the M-SSF system and qualitatively characterized the biological process of water purification. However, to better characterize the environmental functions of microorganisms present in epikarst

spring waters, further research such as metagenomic sequencing or macro-transcriptome sequencing should be done. In addition, further research on genes encoding enzymes involved in nitrogen metabolism (e.g., ammonia monooxygenases, nitrite reductases, and nitrous oxide reductases) in the schmutzdecke might be helpful to understand the purification mechanism of nitrate and ammonia in SSF (Braker *et al.* 1998; Moore *et al.* 2011; Zhou *et al.* 2011; Yang *et al.* 2019).

CONCLUSION

The results presented here highlight the high level of sensitivity epikarst spring water experience with regards to pollution from human activity, and outline an effective, simple, and affordable SSF system based on MHRCCCL for treatment of these epikarst spring water sources upon which local communities are dependent. This paper makes good strides to characterize the microbial community that establishes itself in the SSF and shows a meaningful relationship between bacterial and protozoan communities, which provides new evidence for SSF to build a closed food chain responsible for the improvement in the safety of drinking water. A more in-depth study of how the communities are established could yield a better understanding of how the critical functions are delivered.

ACKNOWLEDGEMENTS

This research was supported by the (1) Natural Science Foundation of Hebei Province (C2020504001), (2) National Key R&D Program of China (2016YFC0502502), (3) China Geological Survey (DD20190356 and DD20189262), (4) Chinese Academy of Geological Sciences (YKWF201628), and (5) National Natural Science Foundation of China (No. 41272301).

DATA AVAILABILITY STATEMENT

All relevant data are included in the paper or its Supplementary Information.

REFERENCES

- Ahmed, W., Gardner, T. & Toze, S. 2011 Microbiological quality of roof-harvested rainwater and health risks: a review. *Journal of Environment Quality* **40** (1), 13–21.
- Bai, Y., Liu, R., Liang, J. & Qu, J. 2013 Integrated metagenomic and physiochemical analyses to evaluate the potential role of microbes in the sand filter of a drinking water treatment system. *PLoS One* **8** (4), e61011.
- Bakalowicz, M. 2004 The epikarst, the skin of karst. *Karst Waters Institute Special Publication* **9**, 16–22.
- Bandy, A. M., Cook, K., Fryar, A. E. & Zhu, J. 2020 Differential transport of *Escherichia coli* isolates compared to abiotic tracers in a karst aquifer. *Ground Water* **58** (1), 70–78.
- Bauer, R., Dizer, H., Graeber, I., Rosenwinkel, K. H. & Lopez-Pila, J. M. 2011 Removal of bacterial fecal indicators, coliphages and enteric adenoviruses from waters with high fecal pollution by slow sand filtration. *Water Research* **45** (2), 439–452.
- Braker, G., Andreas, F. & Witzel, K.-P. 1998 Development of PCR primer systems for amplification of nitrite reductase genes (*nirK* and *nirS*) to detect denitrifying bacteria in environmental samples. *Applied and Environmental Microbiology* **64** (10), 3769–3775.
- Champollion, C., Deville, S., Chéry, J., Doerflinger, E., Le Moigne, N., Bayer, R., Vernant, P. & Mazzilli, N. 2018 Estimating epikarst water storage by time-lapse surface-to-depth gravity measurements. *Hydrology and Earth System Sciences* **22** (7), 3825–3839.
- Chen, H., Zhao, J., Zhong, A. & Jin, Y. 2011 Removal capacity and adsorption mechanism of heat-treated palygorskite clay for methylene blue. *Chemical Engineering Journal* **174** (1), 143–150.
- D'Alessio, M., Yoneyama, B., Kirs, M., Kisand, V. & Ray, C. 2015 Pharmaceutically active compounds: their removal during slow sand filtration and their impact on slow sand filtration bacterial removal. *Science of the Total Environment* **524**, 124–135.
- Deeg, C. M., Emma George, M. M. Z., Husnik, F., Keeling, P. J. & Suttle, C. A. 2018 Chromulinavorax destructans, a pathogenic TM6 bacterium with an unusual replication strategy targeting protist mitochondrion. *BioRxiv* 379–388. <https://doi.org/10.1101/379388>
- Devadhanam Joubert, E. & Pillay, B. 2008 Visualisation of the microbial colonisation of a slow sand filter using an environmental scanning electron microscope. *Electronic Journal of Biotechnology* **11** (2), 119–125.
- Duane, C. & Wolf, H. D. S. 1994 Methods of soil analysis: part 2 – microbiological and biochemical properties. *SSSA Book Series* **5**, 41–51.
- Edgar, R. C. 2013 UPARSE: highly accurate OTU sequences from microbial amplicon reads. *Nature Methods* **10**, 996.
- Ellis, K. V. & Aydin, M. E. 1995 Penetration of solids and biological activity into slow sand filters. *Water Research* **29** (5), 1333–1341.

- Fish, K., Osborn, A. M. & Boxall, J. B. 2017 Biofilm structures (EPS and bacterial communities) in drinking water distribution systems are conditioned by hydraulics and influence discoloration. *Science of the Total Environment* **593**, 571–580.
- Guerrero, C., Mataix-Solera, J., Gómez, I., García-Orenes, F. & Jordán, M. M. 2005 Microbial recolonization and chemical changes in a soil heated at different temperatures. *International Journal of Wildland Fire* **14** (4), 385–400.
- Haig, S. J., Collins, G., Davies, R. L., Dorea, C. C. & Quince, C. 2011 Biological aspects of slow sand filtration: past, present and future. *Water Science and Technology: Water Supply* **11** (4), 468–472.
- Haig, S. J., Quince, C., Davies, R. L., Dorea, C. C. & Collins, G. 2014 Replicating the microbial community and water quality performance of full-scale slow sand filters in laboratory-scale filters. *Water Research* **61**, 141–151.
- Haig, S., Quince, J., Davies, C., Dorea, R. L. & Collins, C. C. G. 2015 The relationship between microbial community evenness and function in slow sand filters. *MBio* **6** (5), e00729–15.
- He, X. & Li, Q. 2005 Hydrochemical variations of the epikarst zone its environmental effects: an example spring of Landiantang at Nongla, Mashan. *Journal of Guangxi Normal University* **23** (2), 103–106 (in Chinese).
- He, Z., Liang, H., Yang, Z., Huang, F. & Zeng, X. 2018 Water system characteristics of Karst river basins in South China and their driving mechanisms of hydrological drought. *Natural Hazards* **92** (2), 1155–1178.
- Hu, K., Chen, H., Nie, Y. & Wang, K. 2015 Seasonal recharge and mean residence times of soil and epikarst water in a small karst catchment of southwest China. *Scientific Reports* **5**, 10215.
- Jenkins, M. W., Tiwari, S. K. & Darby, J. 2011 Bacterial, viral and turbidity removal by intermittent slow sand filtration for household use in developing countries: experimental investigation and modeling. *Water Research* **45** (18), 6227–6239.
- Jiang, Y., Zhang, C., Yuan, D., Zhang, G. & He, R. 2008 Impact of land use change on groundwater quality in a typical karst watershed of southwest China: a case study of the Xiaojiang watershed, Yunnan Province. *Hydrogeology Journal* **16** (4), 727–735.
- Kalyuzhnaya, M. G., Bowerman, S., Lara, J. C., Lidstrom, M. E. & Chistoserdova, L. 2006 *Methylotenera mobilis* gen. nov., sp. nov., an obligately methylamine-utilizing bacterium within the family Methylophilaceae. *International Journal of Systematic and Evolutionary Microbiology* **56** (Pt 12), 2819–2823.
- Kampfer, P., Busse, H. J., Longaric, I., Rossello-Mora, R., Galatis, H. & Lodders, N. 2012 *Pseudarcicella hirusinis* gen. nov., sp. nov., isolated from the skin of the medical leech *Hirudo medicinalis*. *International Journal of Systematic and Evolutionary Microbiology* **62** (Pt 9), 2247–2251.
- Lautenschlager, K., Hwang, C., Ling, F., Liu, W. T., Boon, N., Köster, O., Egli, T. & Hammes, F. 2014 Abundance and composition of indigenous bacterial communities in a multi-step biofiltration-based drinking water treatment plant. *Water Research* **62**, 40–52.
- Lee, E. & Oki, L. R. 2013 Slow sand filters effectively reduce *Phytophthora* after a pathogen switch from *Fusarium* and a simulated pump failure. *Water Research* **47** (14), 5121–5129.
- Li, Q., Sun, H., Han, J., Liu, Z. & Yu, L. 2007 High-resolution study on the hydrochemical variations caused by the dilution of precipitation in the epikarst spring: an example spring of Landiantang at Nongla, Mashan, China. *Environmental Geology* **54** (2), 347–354.
- Liu, Z. P., Wang, B. J., Liu, Y. H. & Liu, S. J. 2005 *Novosphingobium taihuense* sp. nov., a novel aromatic-compound-degrading bacterium isolated from Taihu Lake, China. *International Journal of Systematic and Evolutionary Microbiology* **55** (Pt 3), 1229–1232.
- Mi, Z., Dai, Y., Xie, S., Chen, C. & Zhang, X. 2015 Impact of disinfection on drinking water biofilm bacterial community. *Journal of Environmental Sciences* **37**, 200–205.
- Moore, T. A., Xing, Y., Lazenby, B., Lynch, M. D., Schiff, S., Robertson, W. D., Timlin, R., Lanza, S., Ryan, M. C., Aravena, R., Fortin, D., Clark, I. D. & Neufeld, J. D. 2011 Prevalence of anaerobic ammonium-oxidizing bacteria in contaminated groundwater. *Environmental Science & Technology* **45** (17), 7217–7225.
- Oh, S., Hammes, F. & Liu, W. T. 2018 Metagenomic characterization of biofilter microbial communities in a full-scale drinking water treatment plant. *Water Research* **128**, 278–285.
- Pipan, T., Culver, D. C., Papi, F. & Kozel, P. 2018 Partitioning diversity in subterranean invertebrates: the epikarst fauna of Slovenia. *PLoS One* **13** (5), e0195991.
- Pronk, M., Goldscheider, N., Zopfi, J. & Zwahlen, F. 2009 Percolation and particle transport in the unsaturated zone of a karst aquifer. *Ground Water* **47** (3), 361–369.
- Ren, R., Yang, C. & Kuang, Y. 2018 Study on exploitation model of epikarst spring karst water Wumengshan area. *Ground Water* **40** (2), 24–26 (in Chinese).
- Saifullah, D. H. & Purnomo, B. H. 2015 Water quality of Situ Cibanten based on Shannon-Weaver diversity index value. *Jurnal Perikanan dan Kelautan* **5** (1), 1–4.
- Savio, D., Stadler, P., Reischer, G. H., Demeter, K., Linke, R. B., Blaschke, A. P., Mach, R. L., Kirschner, A. K. T., Stadler, H. & Farnleitner, A. H. 2019 Spring water of an alpine karst aquifer is dominated by a taxonomically stable but discharge-responsive bacterial community. *Frontiers in Microbiology* **10**, 28.
- Sun, Y., Zhang, S., Lan, J., Xie, Z., Pu, J., Yuan, D., Yang, H. & Xing, B. 2019 Vertical migration from surface soils to groundwater and source appointment of polycyclic aromatic hydrocarbons in epikarst spring systems, southwest China. *Chemosphere* **230**, 616–627.

- Trček, B. 2006 How can the epikarst zone influence the karst aquifer hydraulic behaviour? *Environmental Geology* **51** (5), 761–765.
- Wang, Y., Yuan, D. & Yang, S. 2005 Effective exploitation model of karst water in Xiaojiang Basin, Luxi County, Yunnan. *Carsologica Sinica* **24** (4), 305–311 (in Chinese).
- Weber-Shirk, M. L. & Dick, R. I. 1999 Bacterivory by a chrysophyte in slow sand filters. *Water Research* **33** (3), 631–638.
- WHO 2011 *Guidelines for Drinking-Water Quality*, 4th edn. World Health Organization, Geneva, Switzerland.
- Williams, P. W. 2008 The role of the epikarst in karst and cave hydrogeology: a review. *International Journal of Speleology* **37** (1), 1–10.
- Wittebolle, L., Marzorati, M., Clement, L., Balloi, A., Daffonchio, D., Heylen, K., Vos, P. D., Verstraete, W. & Boon, N. 2009 Initial community evenness favours functionality under selective stress. *Nature* **458** (7238), 623–626.
- Wu, P., Tang, C., Zhu, L., Liu, C., Cha, X. & Tao, X. 2009 Hydrogeochemical characteristics of surface water and groundwater in the karst basin, southwest China. *Hydrological Processes* **23** (14), 2012–2022.
- Yang, H., Zhang, G., Yang, X., Wu, F., Zhao, W., Zhang, H. & Zhang, X. 2017 Microbial community diversity and differences in cellar water of typical rainwater harvesting area. *Environmental Science* **38** (11), 4733–4747 (in Chinese).
- Yang, X. C., Han, Z. Z., Ruan, X. Y., Chai, J., Jiang, S. W. & Zheng, R. 2019 Composting swine carcasses with nitrogen transformation microbial strains: succession of microbial community and nitrogen functional genes. *Science of the Total Environment* **688**, 555–566.
- Yun Kit Yeoh, Y. S., Parks, D. H. & Hugenholtz, P. 2016 Comparative genomics of candidate phylum TM6 suggests that parasitism is widespread and ancestral in this lineage. *Molecular Biology and Evolution* **33** (4), 915–927.
- Zelaya, A. J., Parker, A. E., Bailey, K. L., Zhang, P., Van Nostrand, J., Ning, D., Elias, D. A., Zhou, J., Hazen, T. C., Arkin, A. P. & Fields, M. W. 2019 High spatiotemporal variability of bacterial diversity over short time scales with unique hydrochemical associations within a shallow aquifer. *Water Research* **164**, 114917.
- Zhang, G., Zhao, L., Wu, F., Zhang, M., Yue, Z., Wang, Q., Yang, S., Wang, J. & Gong, S. 2017 Study on rough filtration plus slow sand filtration techniques for cellar water of villages and towns in northwest China. *Advances in Engineering Research* **143**, 154–166.
- Zhao, Z., Shen, Y., Shan, Z., Yu, Y. & Zhao, G. 2018 Infiltration patterns and ecological function of outcrop runoff in epikarst areas of Southern China. *Vadose Zone Journal* **17** (1), 1–10.
- Zhao, Y., Wang, X., Liu, C., Wang, S., Wang, X., Hou, H., Wang, J. & Li, H. 2019 Purification of harvested rainwater using slow sand filters with low-cost materials: bacterial community structure and purifying effect. *Science of the Total Environment* **674**, 344–354.
- Zhou, Z. F., Zheng, Y. M., Shen, J. P., Zhang, L. M. & He, J. Z. 2011 Response of denitrification genes nirS, nirK, and nosZ to irrigation water quality in a Chinese agricultural soil. *Environmental Science and Pollution Research International* **18** (9), 1644–1652.
- Zhu, S. 2014 *The Experimental Study of Modified Filter Media for Cellar Water Treatment Using Biology Slow Filtering Techniques*. Lanzhou Jiaotong University, Lanzhou, China (in Chinese).
- Zipf, M. S., Pinheiro, I. G. & Conegero, M. G. 2016 Simplified greywater treatment systems: slow filters of sand and slate waste followed by granular activated carbon. *Journal of Environmental Management* **176**, 119–127.
- Zou, S., Li, Z., Chen, H., Liang, B. & Xia, R. 2007 A preliminary discussion on the pollution of dispersed water supply in southwest Karst Area. *Resources and Environment in the Yangtze Basin* **16** (2), 240–244 (in Chinese).

First received 25 September 2020; accepted in revised form 22 January 2021. Available online 11 February 2021